JOURNAL OF AIRCRAFT
Vol. 34, No. 5, September–October 1997

Dynamic Leading-Edge Flap Scheduling

R. M. Rennie*
Aiolos Engineering Corporation, Toronto, Ontario M9W 1K4, Canada
and
E. J. Jumper†
University of Notre Dame, Notre Dame, Indiana 46556-5684

This paper reports on an experimental determination of a leading-edge flap schedule used to maintain attached flow during arbitrary dynamic pitch motions of a NACA 0009 airfoil. The airfoil could be made to dynamically pitch about its midchord, and was equipped with a 20% leading-edge flap and 27% trailing-edge flap, both of which could be independently and dynamically deflected. Airfoil normal force histories were measured during dynamic pitch and/or flap motions (either or both flaps) by integrating the time histories of pressure measurements taken at 28 locations enveloping the airfoil. A static leading-edge flap schedule was determined using both flow visualization and surface pressure surveys; it was found that attached flow could be maintained by keeping the leading-edge flap aligned with the oncoming flow. Application of the statically determined leading-edge flap schedule during dynamic airfoil or combined airfoil and trailing-edge flap motions showed that this simple leading-edge flap schedule worked even more robustly during dynamic experiments. Finally, the leading-edge flap schedule was applied to an unsteady lift-control experiment, in which trailing-edge flap motions computed using a control algorithm were used to control the unsteady lift on the airfoil during large dynamic pitch motions. These experiments showed that satisfactory lift control was possible when the leading-edge flap schedule was implemented, and that no modification to the lift-control algorithm was necessary to account for the leading-edge flap motions.

Nomenclature

b = airfoil semichord, $c/2$
C_l = lift coefficient
C_n = normal force coefficient
c = airfoil chord
f = frequency
k = reduced frequency, $2\pi fb/V_\infty$
V_∞ = freestream velocity
α = angle of attack
α = nondimensional pitch rate, $\alpha^* b/V_\infty$
δ_{LE} = leading-edge flap deflection angle
δ_{TE} = trailing-edge flap deflection angle

Superscript
* = dimensional quantities

I. Introduction

STEADY mission adaptive wing configurations have and continue to be investigated in an attempt to optimize wing loading, drag, and separation characteristics for sustained flight conditions.[1–3] Significant drag reductions at relatively high C_l values have been demonstrated by Ferris,[1] for example, for low-thickness-ratio wings by adjusting twist and camber via a relatively complex leading- and trailing-edge segmented flap system. In essence, these camber-adjusting techniques effect a redistribution of the steady pressure distribution over the suction surface of the airfoil to favor attached flow at angles of attack that would normally lead to regions of separation and/or stall. In general, the most readily adaptable wing geometries are simple hinged leading- and trailing-edge flaps. The use of adjusted leading/trailing-edge flap positions, camber-scheduling, during specific sustained flight regimes is, in fact, commonly used in some high-performance aircraft to extend range. It is well known that static deflection of a leading-edge flap can be used to delay boundary-layer separation from the suction side of an airfoil to higher angles of attack by decreasing the severity of the adverse pressure gradient.[4,5]

In the case of dynamic flight maneuvers, leading-edge flaps offer the same boundary-layer-control potential for suppressing suction-surface separation and stall. There are two classes of issues involved in attempting to determine a separation-control leading-edge flap schedule for dynamic maneuvers: the first is that it has now been established that even at relatively low reduced rates, the unsteady flow affects the development of the boundary layer and subsequent separation of the flow.[6–8] Secondly, at higher reduced rates, the aerodynamic response of the airfoil is dependent not only on α, and/or δ_{LE} and δ_{TE}, but also on the first and second derivatives of α, δ_{LE}, δ_{TE}. Thus, determining and implementing such a dynamic-flap schedule could be complicated. Once determined, however, a dynamic leading-edge flap schedule could allow high-performance aircraft to achieve rapid and sustained high C_l, above that achievable for nonflapped airfoils. Such higher C_l could be used to enhance maneuverability in a more predictable and sustainable manner than schemes that had been proposed by possible exploitation of dynamic stall[9]; research indicates that dynamic-stall exploitation provides only transient enhancement, and that sustained, time-averaged C_l enhancement is achievable only through suppression of dynamic separation.[6]

Dynamic leading-edge flap scheduling could also lead to enhanced aircraft agility[10] through dynamic lift-control and lift-suppression schemes that depend on dynamic trailing-edge-flap motions.[7,8,11] Dynamic trailing-edge-flap lift control has been shown to be reasonably successful[7,8]; however, robust control depends on the flow over the suction side of the air-

Presented as Paper 95-1904 at the AIAA 13th Applied Aerodynamics Conference, San Diego, CA, June 19–22, 1995; received Sept. 29, 1996; revision received March 26, 1997; accepted for publication March 26, 1997.

*Aerodynamicist. Member AIAA.
†Associate Professor, Hessert Center for Aerospace Research, Department of Aerospace and Mechanical Engineering. Associate Fellow AIAA.

foil/flap remaining attached. Without employing some kind of boundary-layer control, the ability to control lift during rapid pitch up/down maneuvers has been limited to maximum angles of attack of less than approximately 8 deg for the relatively thin airfoils associated with high-performance aircraft.

This paper reports on research directed toward determining a robust, dynamic leading-edge flap schedule for suppressing suction-surface separation during rapid, arbitrary airfoil pitching maneuvers for the purpose of either enhancing C_l or controlling/suppressing C_l via dynamic trailing-edge flap deflections.

A. Unsteady Boundary-Layer Separation Issues

Previous studies have demonstrated that unsteady angle-of-attack motions[6,12] and unsteady flap motions[7,8] tend to suppress separation on the suction surface of the airfoil and/or flap to higher angles of attack and flap deflections than possible in steady flow. Thus, it might reasonably be expected that any leading-edge flap schedule that delays separation in steady flow should not only work under dynamic conditions, but also function more robustly. In this sense, then, the work reported here began with the supposition that a reasonable starting point for dynamic leading-edge flap scheduling should begin by determining the steady flap schedule that suppresses separation to the highest possible angle of attack, over the widest range of trailing-edge flap deflections. Extension of the static leading-edge flap schedule to the dynamic case would then give a dynamic leading-edge flap schedule that depended on both the instantaneous α and the instantaneous δ_{TE}. As mentioned earlier, the dynamic leading-edge flap schedule might also depend on the first and second derivatives of α and δ_{TE}, as well as the previous motion history of these quantities. The derivatives and motion history questions are related to the unsteady aerodynamic-response issues, to be discussed next; however, based on the discussion in this section, the starting supposition is that the unsteady effects (derivatives and motion history) will tend to make a schedule based on instantaneous α and δ_{TE} more robust.

B. Unsteady Aerodynamic Response Issues

The two issues associated with unsteady aerodynamic response are 1) whether rapid leading-edge flap deflections will elicit concomitant unsteady lift and moment responses, in and of themselves, and 2) whether rapid leading-edge flap deflections will affect already established, unsteady, lift-control algorithms based on dynamic trailing-edge flap motions. It has been shown that the unsteady lift response for arbitrary pitch and flap motions is well characterized by the unsteady, inviscid, planar–wing approximation.[7,8,13–15] The response depends on circulatory and noncirculatory components. Although the noncirculatory components can be important at high nondimensional rates, at the rates considered in the present study, the circulatory components form the major contributors to the unsteady aerodynamic response. It is possible to assess the importance that the unsteady motion of the 20% leading-edge flap used in this study could be expected to have on the overall airfoil's unsteady response by examining the flap's influence on steady lift. As shown in the Appendix, the lift-curve slope for leading-edge flap deflections ($dC_l/d\delta_{LE}$) is only (negative) 4% of the lift-curve slope based on angle of attack ($dC_l/d\alpha$), and (negative) 6% of the lift-curve slope based on trailing-edge flap deflections ($dC_l/d\delta_{TE}$). In steady flow, the circulation can be related directly to the lift through the Kutta–Joukowski theorem; since the unsteady lift history can be built up as a series of indicial, Wagner-function-type impulses, this scaling of the asymptotic circulation ratios should also hold for the unsteady aerodynamic response. Thus, it would seem that the circulatory unsteady lift response caused by rapid leading-edge flap deflections might reasonably be neglected in terms of predicting the unsteady response of the airfoil to rapid angle-of-attack and/or rapid trailing-edge flap motions, whether or not the leading-edge flap is also in motion. As will be addressed in the paper, this expectation was experimentally validated.

C. Approach

With the previous discussion in mind, our approach was to experimentally determine the optimal form of the steady leading-edge flap schedule, as a function of α and δ_{TE}, to assure attached flow over the suction surface of the (20% leading-edge-flapped and 27% trailing-edge-flapped) airfoil to the highest possible angle of attack. This was done in two ways: 1) using smoke flow visualization[16] and 2) surface pressure distributions. The resulting steady leading-edge flap schedule was then tested under dynamic pitch motions and dynamic lift-control studies where the trailing-edge flap was used to control the lift.

II. Experimental Approach

The present study was part of an experimental investigation into unsteady lift control using dynamic trailing-edge flap motions.[7,8,11] For the investigation, a test rig and motion control system were constructed to enable simultaneous and controlled angle of attack and/or flap motions of an 8-in. chord, NACA 0009 airfoil with a 20% leading-edge flap and a 27% trailing-edge flap. The flaps were plain type, with sealed gaps (Fig. 1). The chord Reynolds number for the experiments, based on the tunnel wind speed of 45 ft/s, was 2×10^5. For dynamic experiments, airfoil angle-of-attack ramp and oscillatory motions were investigated. Angle-of-attack ramp motions were in the 25–300 deg/s range, while oscillations were performed at 0.5–3 Hz. This motion range corresponded to nondimensional rates $\dot{\alpha}$ of 0.003–0.039, and reduced frequencies k of 0.02–0.14, which are comparable to the kinds of nondimensional motion rates investigated in other studies of dynamic maneuvers.[17–19]

Motion-induced, unsteady lift histories were acquired by integrating unsteady pressures measured at 28 locations on the airfoil surface. The airfoil tap locations are included in Fig. 1. The surface-pressure taps were separated from the pressure transducers by approximately 30 in. of 0.05-in. i.d. plastic pressure tubing. The dynamic response of the pressure tubing was measured in an independent test, which showed that the effect of the tubing was to impose a constant time lag on all dynamic pressure signals; for dynamic experiments, this time lag was removed from all measured pressure histories. The corrected pressure histories were then integrated to generate airfoil C_n histories, which were ensembled averaged over 10 runs; an error bar that denotes the 95% precision interval of the C_n data is included with the C_n curves presented. For further details regarding the experimental apparatus and technique, the reader is referred to Refs. 7 and 8.

III. Results

A. Determination of Static Leading-Edge Flap Schedule

The first task was to determine a leading-edge flap schedule that would prevent boundary-layer separation on the airfoil in steady flow. This static leading-edge flap schedule was obtained from both flow visualization data and static surface pressure measurements. Flow visualization data were gathered for trailing-edge flap deflections between ± 20 deg and angles of attack in the range ± 15 deg. For each angle of attack and trailing-edge flap setting, the leading-edge flap was rotated until the smoke showed no apparent separated regions on the

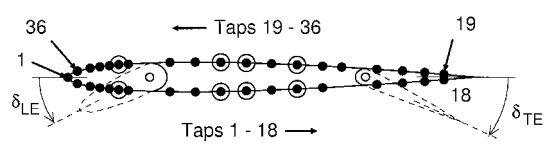

Fig. 1 Diagram of airfoil showing pressure tap locations. Circled taps were excluded from dynamic experiments.

airfoil surface. The range of leading-edge flap deflections over which the flow was attached was recorded in a test log.

The airfoil surface pressure distribution was measured for trailing-edge flap deflections between ±15 deg and airfoil angles of attack between ±15 deg. Each pressure distribution was then evaluated for either attached or separated flow behavior. An example of a pressure distribution that was considered attached is shown in Fig. 2. In this case, a region of flow separation exists (separation bubble) just aft of the sharp edge of the leading-edge flap hinge when the flap is deflected; however, this region was small and, in fact, had not been noticed in the flow-visualization studies. The flow reattaches aft of the region (Fig. 2) from the continued pressure recovery to the trailing edge. The flow over the airfoil at this angle of attack and flap setting was thus considered to be attached. An example of a separated pressure distribution is shown in Fig. 3, which was taken at the same angle of attack as the data of Fig. 2, but without the leading-edge flap deflected. In this case the top surface of the airfoil shows a flat pressure distribution characteristic of separation and stall.

The range of leading-edge flap deflections for which the flow was observed to be attached from flow visualization experiments is plotted in Fig. 4 (dotted line). The trailing-edge flap for the results shown in Fig. 4 was fixed at 0 deg. The results of the surface pressure measurements are included in Fig. 4, where circles represent surface pressure distributions that were judged to be attached, and crosses represent surface pressure distributions that showed boundary-layer separation. Figure 4 shows relatively good agreement between the results of the surface pressure measurements and the flow visualization experiments.

For this study, the leading-edge flap schedules were chosen so as to maintain attached flow over the airfoil throughout the largest possible range of α and δ_{TE} excursions. The leading-edge flap schedule for each trailing-edge flap deflection was determined by performing a linear regression on the mean leading-edge flap angles required for attached flow at each angle of attack. To determine the leading-edge flap schedule

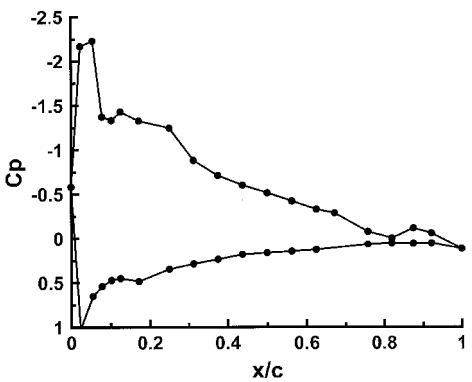

Fig. 2 Example of attached-flow pressure distribution (α = 10 deg, δ_{TE} = 0 deg, δ_{LE} = 10 deg).

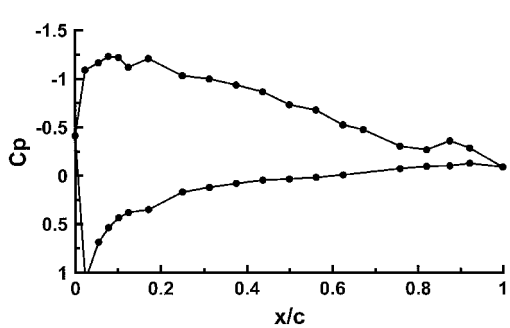

Fig. 3 Example of separated-flow pressure distribution (α = 10 deg, δ_{TE} = 0 deg, δ_{LE} = 0 deg).

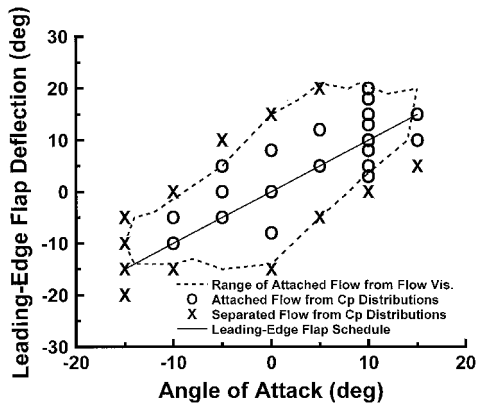

Fig. 4 Leading-edge flap schedule for δ_{TE} = 0 deg.

as a function of both angle of attack and trailing-edge flap deflection, the use of a complicated database formulation was initially considered; however, after examining several leading-edge flap schedules at different trailing-edge flap deflections, it was noticed that the slopes of the fits were all similar, but that the regression constant was a function of trailing-edge flap deflection. As a consequence, the leading-edge flap schedule for any angle of attack and trailing-edge flap deflection was produced by performing a linear regression on the constants at each trailing-edge flap deflection. The equation for the leading-edge flap schedule turned out to be a simple linear algebraic form given by

$$\delta_{LE} = 0.9981\alpha + 0.1948\delta_{TE} \tag{1}$$

where α in Eq. (1) represents the angle of attack of the main airfoil section. The linear form of the leading-edge flap schedule in Eq. (1) agrees with the findings of other investigators; in Ref. 3 an attempt to determine a static leading-edge flap schedule optimized to minimize drag also produced a linear leading-edge flap schedule.

Equation (1) shows that the leading-edge flap deflection required for attached flow depends more strongly on the airfoil angle of attack than on the trailing-edge flap deflection. This result is not unexpected since the size of the airfoil suction peak and, hence, the severity of the adverse pressure gradient on the airfoil, is affected more by the airfoil angle of attack than by trailing-edge flap deflections. Because of this strong dependence of the leading-edge flap schedule on the airfoil angle of attack, the following simplified leading-edge flap schedule was proposed:

$$\delta_{LE} = \alpha \tag{2}$$

This simplification of the leading-edge flap schedule was justified for two reasons. First, the leading-edge flap schedule of Eq. (2) is extremely easy to implement, since it requires only that the leading-edge flap be aligned with the direction of the freestream at all angles of attack. For our apparatus, the leading-edge flap could be so aligned by mechanically clamping the flap, thus removing the need for leading-edge-flap motion control. It was therefore felt that the simplicity of Eq. (2) outweighed any loss of leading-edge flap performance caused by elimination of the trailing-edge flap dependence. Second, for the airfoil used in our study, it was found that the effectiveness of the trailing-edge flap rapidly decreased at large deflections, such that the C_n vs δ_{TE} curve became nonlinear for flap deflections greater than ±10 deg. For this reason, trailing-edge flap deflections were limited to a maximum of around 20 deg. Elimination of the trailing-edge flap dependence from Eq. (1) therefore results in a maximum leading-edge-flap angle error of approximately 4 deg, which was felt to be an acceptable error given the width of the attached flow envelope as shown,

for example, in Fig. 4. The leading-edge flap schedule, Eq. (2), is included in Fig. 4 (solid line).

B. Static C_n vs α Lift Curves

Static C_n vs α curves are shown in Fig. 5 for trailing-edge flap deflections of 0 deg and ± 10 deg, with and without the leading-edge flap following the schedule given in Eq. (2). For the curves shown in Fig. 5, the angle of attack given is that of the main airfoil section, rather than the mean camber line. Although, as discussed earlier, thin-airfoil theory predicts a 4% reduction in lift-curve slope (c.f. previous discussion and the Appendix), Fig. 5 shows that the only effect of the leading-edge flap is to delay the angle of attack at which the airfoil stalls.

C. Extension of Static Leading-Edge Flap Schedule to Dynamic Pitch Motions

The next step in our investigation was to determine if the leading-edge flap schedule, derived under static conditions, would work during dynamic pitch motions. This was investigated using a combination of flow visualization tests and unsteady C_n measurements.

Visualization of the flow around the airfoil was performed using kerosene smoke during sinusoidal pitch motions of the airfoil about its midchord. These tests showed that the leading-edge flap schedule kept the flow attached dynamically at angles of attack that were separated during static tests. For example, Figs. 6a and 6b show flow visualization on the airfoil at the same angle of attack during static and dynamic deflection, respectively, where the dynamic picture was taken during a pitch oscillation of the airfoil at a reduced frequency k of 0.14. In both cases the leading-edge flap is deflected according to the schedule of Eq. (2). Figures 6a and 6b show that the flow separates from the leading-edge flap hinge during static deflection, but remains attached during dynamic oscillation through the same angle of attack. As discussed earlier, this more robust performance of the leading-edge flap schedule under dynamic conditions had been anticipated based on previous work.[6–8,12]

Airfoil normal force C_n histories were acquired for ramp and sawtooth motions of the airfoil. The C_n histories measured during a ramped pitch motion of the airfoil, with the leading-edge flap fixed at 0-deg deflection, and with the leading-edge flap moving according to Eq. (2), are compared in Fig. 7. The figure shows that the two C_n histories are essentially identical, following the same lift-curve slope, up until a time of approximately 0.3 s, at which point a dynamic stall event[9,12] is observed in the history for which the leading-edge flap was undeflected. On the other hand, the C_n history for the case in which the leading-edge flap schedule was implemented shows no evidence of dynamic flow separation. A similar comparison of C_n histories, with and without the leading-edge flap moving according to the schedule, is given for a sawtooth motion in Fig. 8, which also shows that attached flow is maintained using the leading-edge flap. The near-identical behavior of the unsteady aerodynamic responses of the flap-fixed and the flap-scheduled cases while the flow is attached (Figs. 7 and 8), confirms the supposition, discussed earlier, that the unsteady response should be little affected by leading-edge flap motion.

The dynamic flow visualization and unsteady normal-force measurements, therefore, showed that the leading-edge flap schedule developed from static tests was at least as effective, if not more so, at maintaining attached flow during dynamic tests. Further, the unsteady normal force histories show that use of the leading-edge flap avoids catastrophic separation

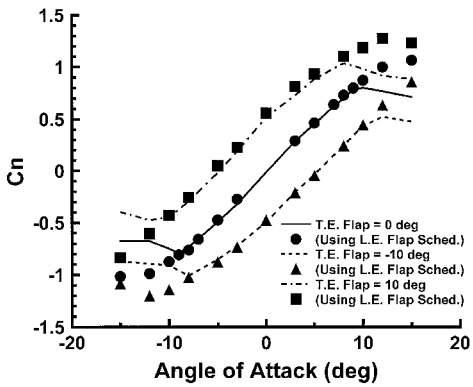

Fig. 5 Static lift curves, with and without leading-edge flap schedule.

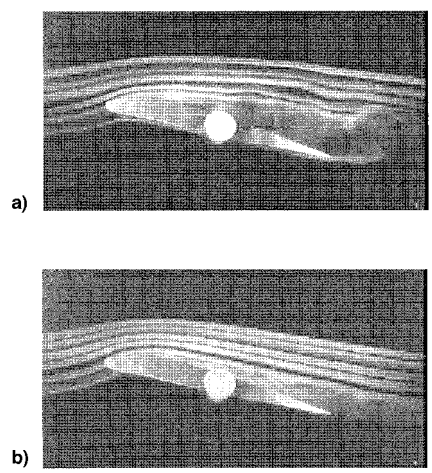

Fig. 6 a) Visualization of flow over airfoil during static deflection and b) during sinusoidal oscillation at reduced frequency k of 0.14 (α = 15 deg in both photographs).

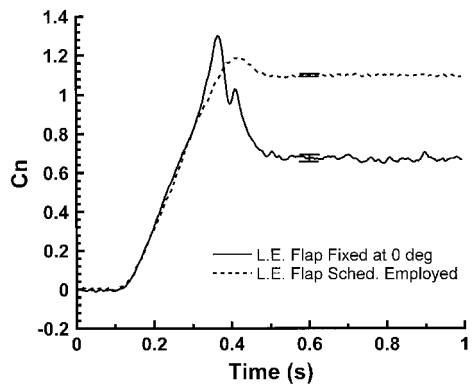

Fig. 7 C_n histories for angle-of-attack ramp, with and without leading-edge flap schedule employed.

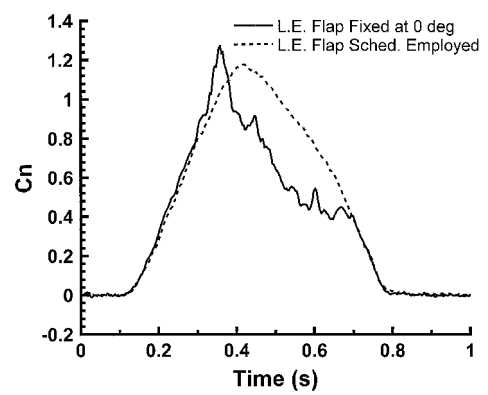

Fig. 8 C_n histories for angle-of-attack sawtooth motion, with and without leading-edge flap schedule employed.

events such as dynamic stall, and results in unsteady lift histories that are robustly repeatable and well behaved.

D. Lift Control of Large-Amplitude Pitch Motions

Unsteady lift-control experiments were performed in an attempt to negate (i.e., control to zero lift) the unsteady lift caused by ramped pitch motions to 15-deg angle of attack, and to negate the unsteady lift during sawtooth pitch motions to a maximum angle of attack of 15 deg. The primary objective of the lift-control experiments was to investigate the effect of leading-edge flap motions on the ability to control the unsteady lift; however, by controlling to zero lift, the motions might be considered representative of point and shoot maneuvers, in which the aircraft fuselage is rotated to aim weapons, and unsteady lift control is employed in an attempt to maintain the aircraft's original trajectory.

The results for a lift-control experiment of a ramped pitch motion to 15-deg angle of attack at a nondimensional rate α of 0.006 are shown in Fig. 9 (employing the leading-edge flap schedule) and in Fig. 10 (leading-edge flap fixed at 0-deg deflection). The first (upper) curve in Fig. 9 shows the unsteady C_n history of the airfoil with the leading-edge flap moved according to the schedule [Eq.(2)], but with the trailing-edge flap fixed at 0-deg deflection. The second (lower) curve shows the C_n history caused by the same airfoil motion and leading-edge flap schedule, but now with the trailing-edge flap deflected according to the algorithm-determined motion required to negate the unsteady lift of the airfoil. Figure 9 shows that the unsteady C_n of the airfoil is successfully negated for the initial part of the experiment, but that the unsteady C_n increases starting at a time of approximately 0.3 s, asymptoting to a final value of 0.5. This departure from zero-lift control is because the trailing-edge flap deflection required to negate the airfoil lift is so large that the effectiveness of the flap [i.e., $(dC_n/d\delta_{TE})$] is reduced by the thickening or separation of the boundary layer on the trailing-edge flap.[7,8] The departure from zero-lift control, however, occurs in a controlled fashion. The results for the same lift control experiment performed with the leading-edge flap fixed at 0-deg deflection are shown in Fig. 10, where, as before, the upper and lower curves show, respectively, the C_n history with and without the trailing-edge flap deflecting to negate the lift on the airfoil. The lower curve in Fig. 10 shows that the unsteady lift on the airfoil is negated successfully until a time of approximately 0.30 s, at which point a large spike in the lift history occurs, and the lift is no longer controlled. As in the uncontrolled case, this lift spike represents a dynamic stall event. Note that comparison of the no-control C_n history to the controlled history shows that the motion of the trailing-edge flap appears to delay the occurrence of dynamic stall on the airfoil.

A similar comparison of controlled and uncontrolled C_n histories for a sawtooth pitch motion is given in Figs. 11 and 12. Figure 11 shows that the lift of the sawtooth motion is successfully negated when the leading-edge flap schedule is employed, except for the time when the effectiveness of the trailing-edge flap is reduced because of the thickening/separation of the boundary layer over the lower surface of the trailing-edge flap. On the other hand, Fig. 12 shows that an attempt to negate the lift during the sawtooth motion without using the leading-edge flap results in a catastrophic dynamic stall event and subsequent loss of control.

The results of this section show that implementation of the dynamic leading-edge flap schedule permits successful control of the unsteady lift on an airfoil undergoing large-amplitude pitch motions. The failure to completely negate the unsteady lift during the airfoil angle-of-attack ramp and sawtooth motions shown in Figs. 9 and 11 was caused by a loss of effectiveness of the trailing-edge flap at large deflection angles; however, the departure from negated lift control in these instances occurred in a controlled manner, in the sense that the

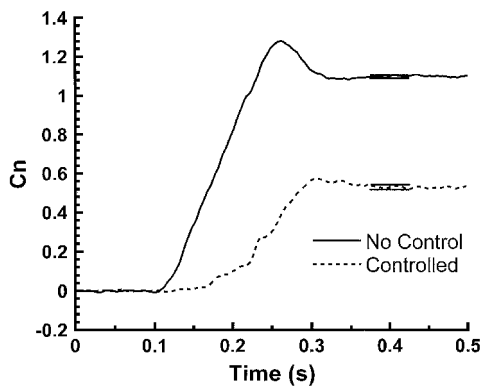

Fig. 9 C_n histories for lift-control of angle-of-attack ramp, with leading-edge flap schedule employed.

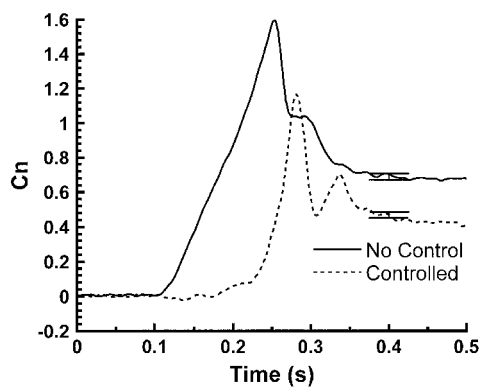

Fig. 10 C_n histories for lift-control of angle-of-attack ramp, with leading-edge flap fixed at 0 deg.

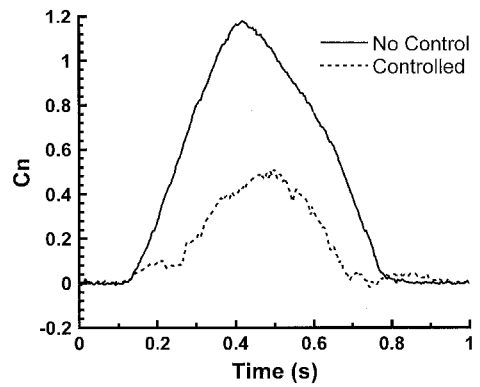

Fig. 11 C_n histories for lift-control of angle-of-attack sawtooth motion, with leading-edge flap schedule employed.

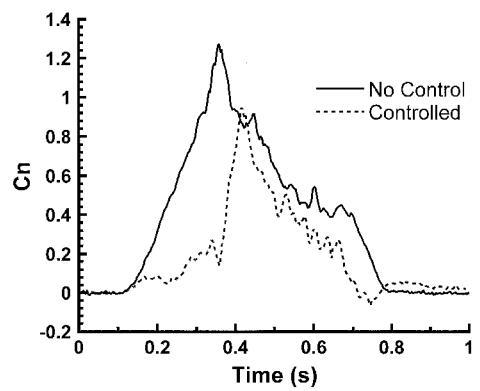

Fig. 12 C_n histories for lift-control of angle-of-attack sawtooth motion, with leading-edge flap fixed at 0 deg.

airfoil boundary layer remained attached throughout the maneuver. As such, it is likely that control over the entire motion could have been accomplished using a more effective lift-control device, or by employing a separation-control technique, such as blowing, over the lower surface of the trailing-edge flap. The experiments for which the leading-edge flap was not employed consistently showed a dynamic-stall event that represented a large C_n excursion from the controlled state, followed by a complete loss of lift control.

IV. Conclusions

The experimental data presented in this paper show that a simple leading-edge flap schedule, in which the leading-edge flap is kept aligned with the direction of the oncoming flow, can be successfully employed as a method of dynamic boundary-layer control. As shown in the lift-control section, maintenance of the attached flow state permitted the use of a previously developed lift control algorithm to compute the required trailing-edge flap motions to control the lift on the airfoil during large-amplitude pitch motions. Finally, it should be noted that the success of the lift-control algorithm, which was not adjusted to account for possible modification of the noncirculatory or circulatory lift of the trailing-edge flap that might be caused by unsteady leading-edge flap motions, supports our supposition that the leading-edge flap can be regarded purely as a boundary-layer control device during dynamic motions, that is essentially uncoupled from the unsteady lift produced by either angle-of-attack or trailing-edge flap motions.

Appendix: Effect of Leading-Edge Flap Deflections on Static Airfoil Lift

From thin-airfoil theory, it can be shown that the lift coefficient of a cambered airfoil, including the effects of both angle of attack α and camber $[z(x/c)]$, is given by[4]

$$C_l = 2\pi \left[\alpha' + \frac{1}{\pi} \int_0^{\pi} \frac{dz}{dx} (\cos\theta - 1)\, d\theta \right] \tag{A1}$$

The nondimensional chordwise coordinate x/c is related to the variable θ by the transformation

$$x/c = \tfrac{1}{2}(1 - \cos\theta) \tag{A2}$$

For deflections of a leading-edge flap and/or a trailing-edge flap of lengths 20 and 27% of the airfoil chord, respectively, the equation of the slope of the airfoil camber line is

$$\frac{dz}{dx} = \begin{cases} 0.8\delta_{LE} + 0.27\delta_{TE}, & 0 \le \dfrac{x}{c} \le 0.2 \\ -0.2\delta_{LE} + 0.27\delta_{TE}, & 0.2 \le \dfrac{x}{c} \le 0.73 \\ -0.2\delta_{LE} - 0.73\delta_{TE}, & 0.73 \le \dfrac{x}{c} \le 1.0 \end{cases} \tag{A3}$$

where, in Eq. (A3), the small angle approximation has been used. Substitution of Eq. (A3) into Eq. (A1), and using the transformation of Eq. (A2), gives the following equation for the airfoil C_l:

$$C_l = 2\pi(\alpha' + 0.1594\delta_{LE} + 0.3604\delta_{TE}) \tag{A4}$$

From geometrical considerations, it can be shown that the angle of attack of the mean camber line α' is related to the angle of attack of the main airfoil section α by

$$\alpha' = \alpha - 0.2\delta_{LE} + 0.27\delta_{TE} \tag{A5}$$

Substitution of Eq. (A5) into Eq. (A4) gives

$$C_l = 2\pi(\alpha - 0.0405\delta_{LE} + 0.6304\delta_{TE}) \tag{A6}$$

Equation (A6) shows that for leading-edge flap deflections the increase in lift because of camber almost cancels the decrease in lift caused by the reduction in the angle of attack of the mean camber line. As such, the lift-curve slope for leading-edge flap deflections is only 4% of the lift-curve slope of the airfoil, and it is 6.4% of that for the trailing-edge flap. Substitution of the leading-edge flap schedule [Eq.(2)], into Eq. (A6) shows that the effect of the leading-edge flap schedule is a reduction in the angle-of-attack lift-curve slope by 4%.

Acknowledgments

This work was supported by the University of Notre Dame, Department of Aerospace and Mechanical Engineering, and by the McDonnell Douglas Corporation in the early stages of this report. We are appreciative of the technical support provided by Richard E. Boalbey and Wayne Ely of the McDonnell Douglas Corporation. We also thank Michael Swadener and Joel Preston for their invaluable assistance in constructing the test section and instrumentation.

References

[1]Ferris, J. C., "Wind Tunnel Investigation of a Variable Camber and Twist Wing," NASA TN D-8475, Aug. 1977.

[2]Norman, D. C., Gangsaas, D., and Hynes, R. J., "An Integrated Maneuver Enhancement and Gust Alleviation Mode for the AFTI/F-111 MAW [Mission Adaptive Wing] Aircraft," AIAA Paper 83-2217, 1983.

[3]Rajeswari, B., and Prabhu, K. R., "Optimum Flap Schedules and Minimum Drag Envelopes for Combat Aircraft," *Journal of Aircraft*, Vol. 24, No. 6, 1987, pp. 412–414.

[4]McCormick, B. M., *Aerodynamics, Aeronautics, and Flight Mechanics*, Wiley, New York, 1979.

[5]Abbot, I. H., and Von Doenhoff, A. E., *Theory of Wing Sections*, Dover, New York, 1959.

[6]Jumper, E. J., and Stephen, E. J., "Toward Unsteady Lift Augmentation, An Assessment of the Role of Competing Phenomenon in Dynamic Stall," *Proceedings of the 2nd AFOSR Workshop on Unsteady Separated Flows*, 1987.

[7]Rennie, R. M., and Jumper, E. J., "Experimental Measurements of Dynamic Control Surface Effectiveness," *Journal of Aircraft*, Vol. 33, No. 5, 1996, pp. 880–887.

[8]Rennie, R. M., "An Experimental Investigation of Unsteady Lift Control Using Trailing-Edge Flaps," Ph.D. Dissertation, Dept. of Aerospace and Mechanical Engineering, Univ. of Notre Dame, Notre Dame, IN, April 1996.

[9]Lang, J. D., and Francis, M. S., "Unsteady Aerodynamics and Dynamic Aircraft Maneuverability," *Proceedings of the AGARD Symposium on Unsteady Aerodynamics—Fundamentals and Applications to Aircraft Dynamics* (Gottingen, Germany), 1985.

[10]Skow, A. M., "Agility as a Contributer to Design Balance," *Journal of Aircraft*, Vol. 29, No. 1, 1992, pp. 34–46.

[11]Hugo, R., and Jumper, E., "Controlling Unsteady Lift Using Unsteady Trailing-Edge Flap Motions," AIAA Paper 92-0275, Jan. 1992.

[12]Jumper, E. J., Schreck, S. J., and Dimmick, R. L., "Lift-Curve Characteristics for an Airfoil Pitching at Constant Rate," AIAA Paper 86-0117, Jan. 1986.

[13]Bisplinghoff, R. L., Ashley, H., and Halfman, R. L., *Aeroelasticity*, Addison–Wesley, Reading, MA, 1955.

[14]Fung, Y. M., *An Introduction to the Theory of Aeroelasticity*, Dover, New York, 1969.

[15]Drescher, H., "Untersuchungen an einem symmetrischen Tragflugel mit spaltlos angeschlossenem Ruder bei Raschen Aenderungen des Ruderausschlags (ebene Stromung)," *Mitt. Max-Planck-Inst. Stromungs-Forsch.*, Nr. 6, Gottingen, Germany, 1952.

[16]Batill, S. M., Nelson, R. C., and Mueller, T. J., "Smoke Flow Visualization at Transonic and Supersonic Mach Numbers," AIAA Paper 82-0188, Jan. 1982.

[17]Lorber, P. F., and Carta, F. O., "Airfoil Dynamic Stall at Constant Pitch Rate and High Reynolds Number," *Journal of Aircraft*, Vol. 25, No. 6, 1988, pp. 548–556.

[18]Den Boer, R. G., and Cunningham, A. M., "Low-Speed Unsteady Aerodynamics of a Pitching Straked Wing at High Incidence—Part I: Test Program," *Journal of Aircraft*, Vol. 27, No. 1, 1990, pp. 23–30.

[19]Cunningham, A. M., and Den Boer, R. G., "Low-Speed Unsteady Aerodynamics of a Pitching Straked Wing at High Incidence—Part II: Harmonic Analysis," *Journal of Aircraft*, Vol. 27, No. 1, 1990, pp. 31–41.